Electronic Journal of Qualitative Theory of Differential Equations
2020, No. **17**, 1–11; https://doi.org/10.14232/ejqtde.2020.1.17 www.math.u-szeged.hu/ejqtde/

A study of logistic growth models influenced by the exterior matrix hostility and grazing in an interior patch

Nalin Fonseka, **Jonathan Machado** and **Ratnasingham Shivaji**✉

University of North Carolina at Greensboro, Department of Mathematics and Statistics, Greensboro, NC 27412, USA

Received 31 August 2019, appeared 18 March 2020
Communicated by Péter L. Simon

Abstract. We will analyze the symmetric positive solutions to the two-point steady state reaction-diffusion equation:

$$\begin{aligned}
-u'' &= \begin{cases} \lambda\left[u - \dfrac{1}{K}u^2 - \dfrac{cu^2}{1+u^2}\right]; & x \in [L, 1-L], \\ \lambda\left[u - \dfrac{1}{K}u^2\right]; & x \in (0,L) \cup (1-L, 1), \end{cases} \\
-u'(0) &+ \sqrt{\lambda}\gamma u(0) = 0, \\
u'(1) &+ \sqrt{\lambda}\gamma u(1) = 0,
\end{aligned}$$

where λ, c, K, and γ are positive parameters and the parameter $L \in (0, \frac{1}{2})$. The steady state reaction-diffusion equation above occurs in ecological systems and population dynamics. The above model exhibits logistic growth in the one-dimensional habitat $\Omega_0 = (0, 1)$, where grazing (type of predation) is occurring on the subregion $[L, 1-L]$. In this model, u is the population density and c is the maximum grazing rate. λ is a parameter which influences the equation as well as the boundary conditions, and γ represents the hostility factor of the surrounding matrix. Previous studies have shown the occurrence of S-shaped bifurcation curves for positive solutions for certain parameter ranges when the boundary condition is Dirichlet ($\gamma \longrightarrow \infty$). Here we discuss the occurrence of S-shaped bifurcation curves for certain parameter ranges, when γ is finite, and their evolutions as γ and L vary.

Keywords: differential equations, boundary value problems, logistic growth, exterior matrix hostility, interior grazing, positive solutions.

2020 Mathematics Subject Classification: 34B08, 34B15, 34B18.

✉ Corresponding author.
Emails: g_fonsek@uncg.edu (N. Fonseka), jonathan.Machado@tufts.edu (J. Machado) r_shivaj@uncg.edu (R. Shivaji)

1 Introduction

First, we briefly discuss the history of grazing type models. Recently in [5], authors discussed the following boundary value problem:

$$\begin{cases} -\Delta u = \lambda \left(u - \dfrac{u^2}{K} - \dfrac{cu^2}{1+u^2} \right); & \Omega, \\ \dfrac{\partial u}{\partial \eta} + \sqrt{\lambda} u = 0; & \partial\Omega, \end{cases} \tag{1.1}$$

where $\frac{\partial u}{\partial \eta}$ is the outward normal derivative of u, $\lambda > 0$, $K > 0$, $0 < c < 2$, and Ω is a bounded domain in $\mathbb{R}^N$; $N \geq 1$ with smooth boundary $\partial\Omega$. Here, u is the population density, λ is a positive parameter, and c is the maximum grazing rate. The term $u - \frac{1}{K}u^2$ represents a logistic growth, which means the per capita growth rate is a linear depreciation. The term $\frac{cu^2}{1+u^2}$ represents the rate of grazing by a constant number of grazers (see Figure 1.2). The authors established the occurrence of S-shaped bifurcation curves when parameters c and K satisfy certain conditions. Grazing type models apply to many ecological systems arising in population dynamics such as the dynamics of salmon fish and spruce budworms (see [9] and [12]).

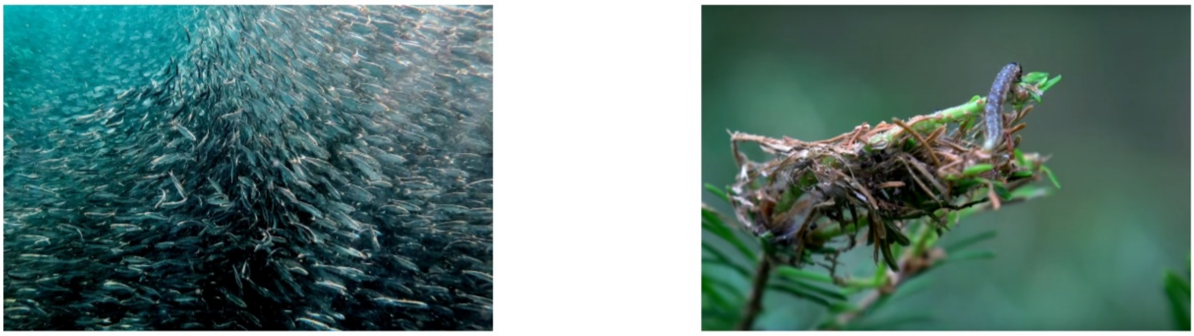

Figure 1.1: Examples of salmon and spruce budworms

However, it turns out that the grazing presents itself only in an interior patch in many real-world situations. We refer the reader to [1] for a study in this direction where the authors studied the following Dirichlet boundary value problem:

$$\begin{aligned} -u'' &= \begin{cases} \lambda \tilde{f}(u); \ x \in [L, 1-L], \\ \lambda f(u); \ x \in (0, L) \cup (1-L, 1), \end{cases} \\ u(0) &= u(1) = 0, \end{aligned} \tag{1.2}$$

where $\tilde{f}(u) = u - \frac{1}{K}u^2 - \frac{cu^2}{1+u^2}$ and $f(u) = u - \frac{1}{K}u^2$, which corresponds to the case where $\gamma \to \infty$ (see (1.5)). Now, λ, c, and K are positive parameters and the parameter $L \in (0, \frac{1}{2})$. The authors showed the occurrence of S-shaped bifurcation curves for certain parameter ranges and numerically obtained the evolution of the bifurcation curves over a range of L-values and K-values, for a fixed value of c. In particular, for $c = 1.5$ they showed that occurrence of S-shaped bifurcation persists for any value of L, if K is chosen to be large enough.

Biologists have recently observed that in the study of grazing models, to better predict the behavior of the ecological system, it is vital to take the exterior matrix hostility factor into

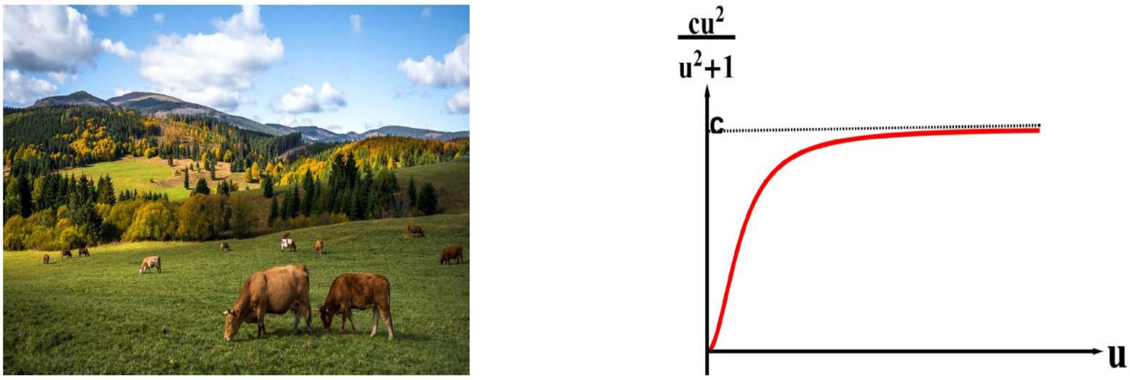

Figure 1.2: Grazing.

account. In this paper, we extend the study in [1] to the case when the exterior matrix hostility is incorporated into the model. We obtain our results via a modified quadrature method and Mathematica computations.

We now briefly discuss the modeling aspect of the problem. We consider the domain $\Omega_0 = \{lx \mid x \in \Omega\}$, where $\Omega = (0,1)$ and l is a parameter representing the size of the habitat. We assume that the diffusion rate in the patch Ω_0 is D. In the matrix $\mathbb{R} \setminus \overline{\Omega}_0$, we assume that the diffusion rate is D_0, and the death rate is S_0.

We will further assume that the population exhibits density dependent dispersal (DDD) on the boundary $\partial\Omega_0$. Defining $\alpha(u)$ as the probability of the population remaining in Ω_0 when it reaches the boundary, the resulting model is (see [2,6,10,11]):

$$\begin{cases} u_t = Du_{xx} + h(u); & x \in \Omega_0, t > 0, \\ u(0,x) = u_0(x); & x \in \Omega_0, \\ D\alpha(u)\dfrac{\partial u}{\partial \eta} + \dfrac{\sqrt{S_0 D_0}}{k}[1-\alpha(u)]u = 0; & x \in \partial\Omega_0, t > 0 \end{cases} \tag{1.3}$$

with the corresponding steady state equation:

$$\begin{cases} -u'' = \dfrac{1}{D}h(u); & x \in \Omega_0, \\ D\alpha(u)\dfrac{\partial u}{\partial \eta} + \dfrac{\sqrt{S_0 D_0}}{k}[1-\alpha(u)]u = 0; & x \in \partial\Omega_0, \end{cases}$$

or equivalently

$$\begin{cases} -u'' = \dfrac{l^2}{D}h(u); & x \in \Omega, \\ \dfrac{\partial u}{\partial \eta} + \dfrac{\sqrt{S_0 D_0}\,l}{kD}\left[\dfrac{1-\alpha(u)}{\alpha(u)}\right]u = 0; & x \in \partial\Omega, \end{cases} \tag{1.4}$$

where k is a positive parameter related to the movement behavior of the species (see [2], [3]). Here $h(u)$ represents the reaction term. More precisely, $h(u) = u - \frac{1}{K}u^2$ in the case of logistic population growth, whereas in the case of logistic growth with grazing $h(u) = u - \frac{1}{K}u^2 - \frac{cu^2}{1+u^2}$. Let $\lambda = \frac{l^2}{D}$ and $\gamma = \frac{\sqrt{S_0 D_0}}{k\sqrt{D}}$. Here γ represents the matrix hostility factor. Then (1.4) reduces to

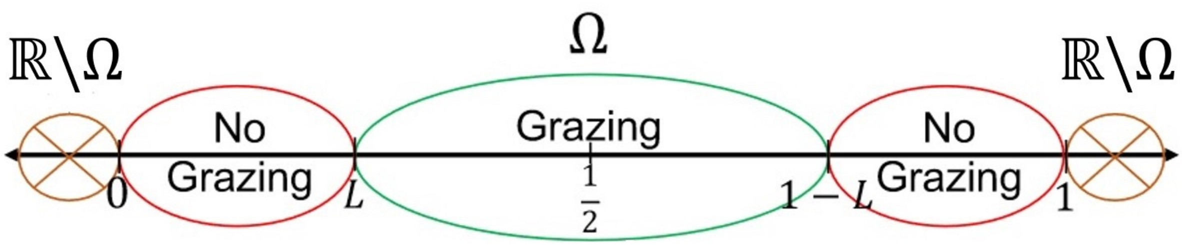

Figure 1.3: Grazing region, non grazing regions and exterior matrix.

$$\begin{cases} -u'' = \lambda h(u); \quad x \in (0,1), \\ -u'(0) + \gamma\sqrt{\lambda}g(u(0))u(0) = 0, \\ u'(1) + \gamma\sqrt{\lambda}g(u(1))u(1) = 0, \end{cases} \tag{1.5}$$

where $g(s) = \frac{1-\alpha(s)}{\alpha(s)}$.

In this paper, we will study positive solutions of (1.5) which are symmetric about $x = \frac{1}{2}$, when $\alpha(s) = \frac{1}{2}$ and

$$h(u) = \begin{cases} \lambda\tilde{f}(u); \ x \in [L, 1-L], \\ \lambda f(u); \ x \in (0, L) \cup (1-L, 1) \end{cases}$$

via a quadrature method. Namely, when $K = 10$ and $c = 1.5$ we will study positive solutions of:

$$\begin{aligned} -u'' &= \begin{cases} \lambda\tilde{f}(u); \ x \in [L, 1-L], \\ \lambda f(u); \ x \in (0, L) \cup (1-L, 1), \end{cases} \\ -u'(0) &+ \gamma\sqrt{\lambda}u(0) = 0, \\ u'(1) &+ \gamma\sqrt{\lambda}u(1) = 0, \end{aligned} \tag{1.6}$$

such that $u(L^-) = u(L^+)$ and $u'(L^-) = u'(L^+)$ where γ is a parameter related to the matrix hostility.

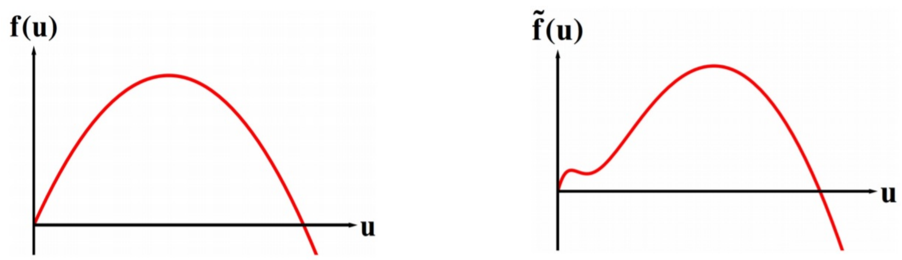

(a) $f(u) = u - \frac{1}{K}u^2$ (b) $\tilde{f}(u) = u - \frac{1}{K}u^2 - \frac{cu^2}{1+u^2}$

Figure 1.4: Shapes of f and $\tilde{f}$.

In particular, we study the evolution of these steady states of (1.6) with respect to L when the hostility parameter γ is fixed and vice-versa.

Now we present the following theorem which describes the structure of such positive solutions.

Let $\|u\|_\infty = \rho$, $u(L) = \sigma$, and $u(0) = u(1) = q$, $\tilde{F}(s) := \int_0^s \tilde{f}(t)dt$ and $F(s) := \int_0^s f(t)dt$.

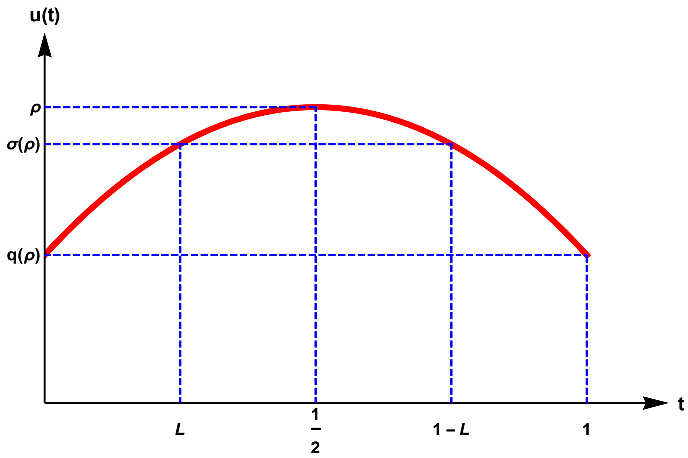

Figure 1.5: Graph of a symmetric solution u to (1.6).

Theorem 1.1. *A symmetric solution (as in Figure 1.5) of (1.6) exists if and only if λ, ρ, σ and q satisfy:*

$$\sqrt{\lambda} = \frac{1}{\sqrt{2}L}\int_q^\sigma \frac{dv}{\sqrt{F(q)+\frac{\gamma^2 q^2}{2}-F(v)}} = \frac{1}{\sqrt{2}(\frac{1}{2}-L)}\int_\sigma^\rho \frac{dv}{\sqrt{\tilde{F}(\rho)-\tilde{F}(v)}},$$
$$F(q)+\frac{\gamma^2 q^2}{2}-F(\sigma) = \tilde{F}(\rho)-\tilde{F}(\sigma).$$

In Section 2, we detail the proof of Theorem 1.1. In Section 3, we provide biological implications and numerical results.

2 Proof of Theorem 1.1

Suppose $u > 0$ is a solution of (1.6). We first focus on the region $(L, \frac{1}{2})$. Multiply both sides of (1.6) by u' and obtain

$$\left[\frac{-(u'(x))^2}{2}\right]' = \lambda\left[\tilde{F}(u(x))\right]'.$$

Next, by integrating, we obtain

$$u'(x) = \sqrt{2\lambda\left[\tilde{F}(\rho)-\tilde{F}(u(x))\right]}; \qquad x \in \left[L, \tfrac{1}{2}\right],$$

and further integration leads to

$$\int_x^{\frac{1}{2}} \frac{u'(s)}{\sqrt{\tilde{F}(\rho)-\tilde{F}(u(s))}}\,ds = \int_x^{\frac{1}{2}} \sqrt{2\lambda}\,ds; \qquad x \in \left[L, \tfrac{1}{2}\right).$$

Now using the substitution $v = u(s)$ we obtain

$$\int_{u(x)}^{u(\frac{1}{2})} \frac{1}{\sqrt{\tilde{F}(\rho)-\tilde{F}(v)}}\,dv = \sqrt{2\lambda}\left[\frac{1}{2}-x\right]; \qquad x \in \left[L, \tfrac{1}{2}\right).$$

Setting $x = L$ we have

$$\int_{\sigma}^{\rho} \frac{1}{\sqrt{\tilde{F}(\rho) - \tilde{F}(v)}}\, dv = \sqrt{2\lambda}\left[\frac{1}{2} - L\right].$$

Further, solving for λ we obtain

$$\lambda = \left[\frac{1}{\sqrt{2}(\frac{1}{2} - L)} \int_{\sigma}^{\rho} \frac{1}{\sqrt{\tilde{F}(\rho) - \tilde{F}(v)}}\, dv\right]^2. \tag{2.1}$$

We next focus on the region $(0, L)$. Again by the above quadrature method, letting $u(0) = q$, by the boundary conditions we get

$$u'(x) = \sqrt{2\lambda\left[F(q) + \frac{\gamma^2 q^2}{2} - F(u(x))\right]}; \qquad x \in [0, L].$$

Integrating on $(0, x)$ we have

$$\int_{q}^{u(x)} \frac{1}{\sqrt{F(q) + \frac{\gamma^2 q^2}{2} - F(v)}}\, dv = \sqrt{2\lambda}x; \qquad x \in [0, L].$$

Hence substituting $x = L$ and solving for λ yields

$$\lambda = \left[\frac{1}{\sqrt{2}L} \int_{q}^{\sigma} \frac{1}{\sqrt{F(q) + \frac{\gamma^2 q^2}{2} - F(v)}}\, dv\right]^2. \tag{2.2}$$

Now using $u'(L^-) = u'(L^+)$, (2.1) and (2.2), we obtain:

$$\frac{1}{\sqrt{2}L} \int_{q}^{\sigma} \frac{dv}{\sqrt{F(q) + \frac{\gamma^2 q^2}{2} - F(v)}} = \frac{1}{\sqrt{2}(\frac{1}{2} - L)} \int_{\sigma}^{\rho} \frac{dv}{\sqrt{\tilde{F}(\rho) - \tilde{F}(v)}}, \tag{2.3}$$

$$F(q) + \frac{\gamma^2 q^2}{2} - F(\sigma) = \tilde{F}(\rho) - \tilde{F}(\sigma). \tag{2.4}$$

In fact, given ρ, q and σ satisfy (2.3) and (2.4), we can back track and use the Implicit Function Theorem to obtain a solution as described in Figure 1.5 with

$$\lambda = \left[\frac{1}{\sqrt{2}L} \int_{q}^{\sigma} \frac{1}{\sqrt{F(q) + \frac{\gamma^2 q^2}{2} - F(v)}}\, dv\right]^2.$$

Hence the proof is complete.

We provide our computational results in the next section.

3 Computational results and biological implications

In [1], authors showed the occurrence of an S-shaped bifurcation curve for (1.2) for certain parameter ranges when grazing is confined to an interior region of $(0, 1)$. Indeed, they numerically showed that for a fixed $c = 1.5$, occurrence of an S-shaped bifurcation curve for (1.2) always happens if K is chosen to be large enough. Namely, they showed that for $K \gg 1$ there exist m_1, m_2, and m_3 such that (1.2) has (see Figure 3.1):

- no positive solution for $\lambda \in (0, m_1]$
- exactly one positive solution for $\lambda \in (m_1, m_2)$
- exactly two positive solutions for $\lambda = m_2$
- exactly three positive solutions for $\lambda \in (m_2, m_3)$
- exactly two positive solutions for $\lambda = m_3$
- exactly one positive solution for $\lambda \in (m_3, \infty)$

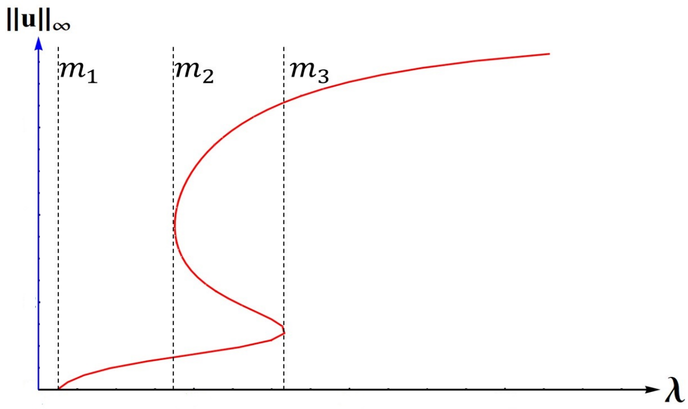

Figure 3.1: Occurrence of S-shaped bifurcation for (1.2).

We will obtain similar results when grazing is restricted to an interior patch, namely for (1.6). Moreover, we investigate the λ region where multiplicity of positive solutions occurs. In particular, we fix all parameters with the exception of L and γ, where variations are implemented. First, we consider fixed values of L, namely $L = 0.05$, 0.30, and 0.45, and we demonstrate the evolution of the bifurcation diagrams for positive solutions when γ varies. Next, for $\gamma = 50$ (fixed), we demonstrate the evolution of the bifurcation diagrams for positive solutions when L varies.

We briefly explain how we obtain numerical bifurcation diagrams. Let $\gamma > 0$, $L > 0$, and $M > 0$ be fixed, and let $x_i = \frac{i}{n+1}$; $i = 1, \ldots, n+1$ for some $n \geq 1$. Letting $\rho = x_1$, we numerically solve the equations (2.3) and (2.4) simultaneously for σ and q using the FindRoot command in Mathematica. The values of σ and q are substituted into (2.2) to find the corresponding value of λ. Repeating this procedure for $\rho = x_i$, $i = 2, \ldots, n+1$, we obtain (λ, ρ) points for the bifurcation diagram.

Our research shows the following four cases:

1) For small values of L, multiplicity of positive solutions persists for certain ranges of λ irrespective of the value of hostility factor.

2) For large values of L, for no ranges of λ multiplicity occurs, regardless of the value of hostility factor.

3) For intermediate values of L, attainment or elimination of multiplicity regions is possible depending on the value of hostility factor.

4) For a fixed $\gamma > 0$, multiplicity regions persist for small L and multiplicity regions are lost for large L.

3.1 Bifurcation diagrams for fixed values of L as γ varies

We closely examine our solutions via extracting the value $E(\gamma)$, where the non-trivial positive solution bifurcates from the trivial branch of solutions, as well as the interval $(A(\gamma, L), B(\gamma, L))$ corresponding to the λ region where multiplicity of positive solutions occurs.
For $L = 0.05$:

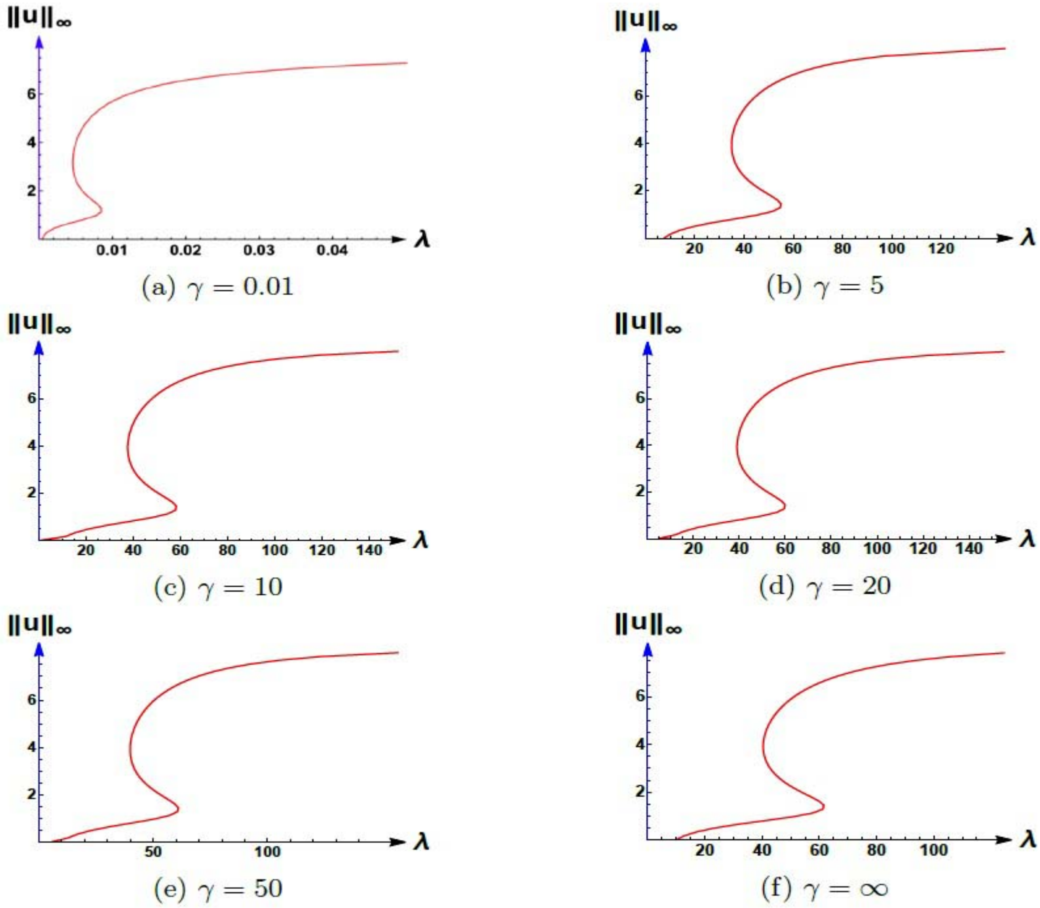

Figure 3.2: Bifurcation diagrams for (1.6) where $K = 10$, $c = 1.5$, and $L = 0.05$.

γ	$E(\gamma)$	$A(\gamma, L)$	$B(\gamma, L)$	$B(\gamma, L) - A(\gamma, L)$
0.01	0.000411825	0.00459959	0.00848834	0.00388875
5	7.66329	34.9839	54.9993	20.0154
10	8.78401	37.6855	58.2939	20.6084
20	9.38331	39.0397	59.946	20.9063
50	9.75404	39.8512	60.937	21.0858
∞	10.0055	40.3913	61.597	21.2057

Table 3.1: Varying γ while $L = 0.05$.

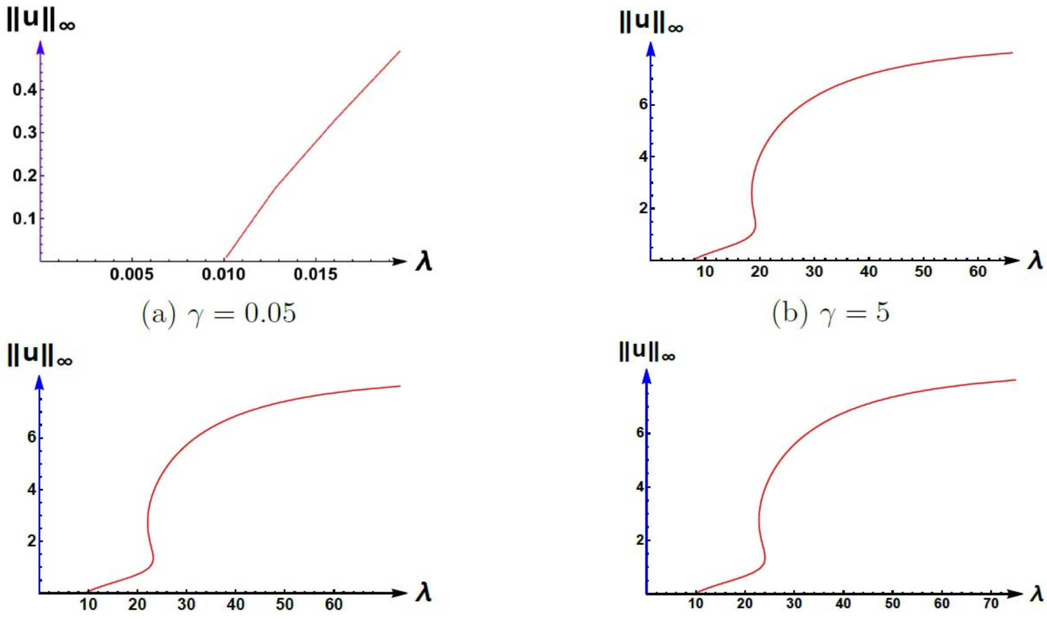

(a) $\gamma = 0.05$ (b) $\gamma = 5$

(c) $\gamma = 20$ (d) $\gamma = 50$

Figure 3.3: Bifurcation diagrams for (1.6) where $K = 10$, $c = 1.5$, and $L = 0.30$.

γ	$E(\gamma)$	$A(\gamma, L)$	$B(\gamma, L)$	$B(\gamma, L) - A(\gamma, L)$
5	7.63138	18.5239	19.2104	0.6865
20	9.35392	22.082	23.2109	1.1289
50	9.72529	22.8384	24.0726	1.2342

Table 3.2: Varying γ while $L = 0.30$.

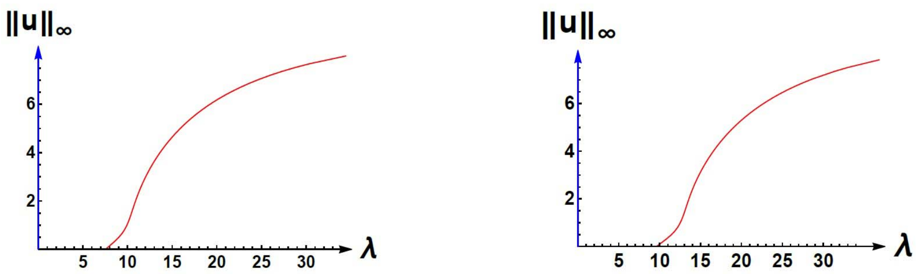

(a) $\gamma = 5$ (b) $\gamma = 50$

Figure 3.4: Bifurcation diagrams for (1.6) where $K = 10$, $c = 1.5$, and $L = 0.45$.

Remark 3.1. Our research concludes that when $K = 10$ and $c = 1.5$ there exists $L_*, L^* \in (0, \frac{1}{2})$ with $L_* < L^*$, such that when $L < L_*$ (grazing in a large subregion), the occurrence of multiple steady states for a range of λ persists for any hostility factor γ, and when $L > L^*$ (grazing in a small subregion), for any hostility factor γ, multiplicity of steady states does not occur for any λ. However, for $L \in (L_*, L^*)$, there exists a $\gamma^*(L) > 0$ such that multiplicity of steady states for a range of λ does occur for any hostility factor $\gamma > \gamma^*(L)$.

3.2 Bifurcation diagrams for a fixed value of γ as L varies

For $\gamma = 50$:

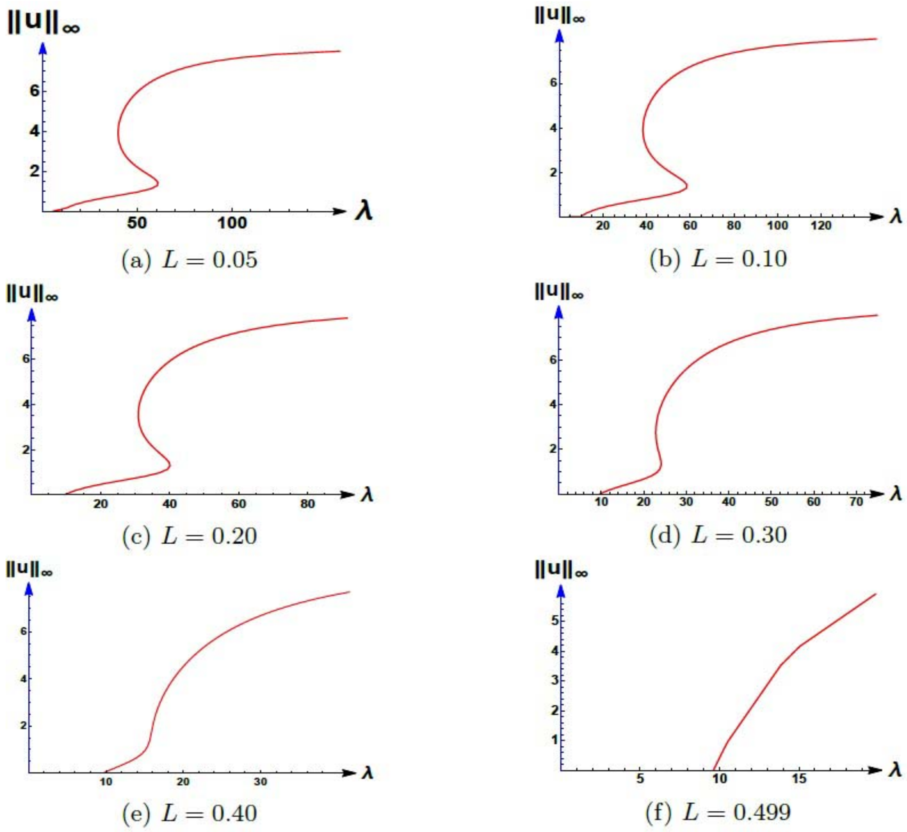

(a) $L = 0.05$ (b) $L = 0.10$ (c) $L = 0.20$ (d) $L = 0.30$ (e) $L = 0.40$ (f) $L = 0.499$

Figure 3.5: Bifurcation diagrams for (1.6) where $K = 10$, $c = 1.5$, and $\gamma = 50$.

L	$E(\gamma)$	$A(\gamma, L)$	$B(\gamma, L)$	$B(\gamma, L) - A(\gamma, L)$
0.01	12.4772	40.0324	59.6438	19.6114
0.10	9.75354	38.3015	58.4055	20.104
0.20	9.74708	30.9087	40.1478	9.2391
0.30	9.72529	22.8384	24.0726	1.2342

Table 3.3: Varying L while $\gamma = 50$.

Remark 3.2. Note that for $\gamma = 50$, when $K = 10$ and $c = 1.5$ the occurrence of multiple positive steady states for a range of λ is lost when L is large (grazing in a small subregion). Furthermore, for any fixed $\gamma > 0$, occurrence of multiple positive steady states for a range of λ are observed for $L \approx 0$ and occurrence of multiple positive steady states for any λ is lost for L large.

Acknowledgment

This material is based upon work supported by the National Science Foundation under Grant No. DMS-1516519.

References

[1] D. Butler, R. Shivaji, A. Tuck, S-shaped bifurcation curves for logistic growth and weak Allee effect growth models with grazing on an interior patch, in: *Proceedings of the Ninth MSU-UAB Conference on Differential Equations and Computational Simulations*, *Electron. J. Differ. Equ. Conf.*, Vol. 20, Texas State Univ., San Marcos, TX 2013, pp. 15–25. MR3128065

[2] J. T. Cronin, Movement and spatial population structure of a prairie planthopper, *Ecology* **84**(2003), No. 5, 1179–1188. https://doi.org/10.1890/0012-9658(2003)084[1179:MASPSO]2.0.CO;2

[3] J. Cronin, J. Goddard, R. Shivaji, Effects of patch-matrix composition and individual movement response on population persistence at the patch-level, *Bull. Math. Biol.* **81**(2019), No. 10, 3933–3975. https://doi.org/10.1007/s11538-019-00634-9; MR4012463

[4] N. Fonseka, J. Goddard, Q. Morris, R. Shivaji, B. Son, On the effects of the exterior matrix hostility and a U-shaped density dependent dispersal on a diffusive logistic growth model, *Discrete Contin. Dyn. Syst. Ser. S*, to appear. https://doi.org/10.3934/dcdss.2020245

[5] N. Fonseka, R. Shivaji, B. Son, K. Spetzer, Classes of reaction diffusion equations where a parameter influences the equation as well as the boundary conditions, *J. Math Anal. Appl.* **476**(2019), No. 2, 480–494. https://doi.org/10.1016/j.jmaa.2019.03.053; MR3958013

[6] J. Goddard II, Q. Morris, C. Payne, R. Shivaji, A diffusive logistic equation with U-shaped density dependent dispersal on the boundary, *Topol. Methods Nonlinear Anal.* **53**(2019), No. 1, 335–349. https://doi.org/10.12775/tmna.2018.047; MR3939159

[7] J. Goddard II, Q. Morris, S. Robinson, R. Shivaji, An exact bifurcation diagram for a reaction diffusion equation arising in population dynamics, *Bound. Value Probl.* **2018**, Paper No. 170, 17 pp. https://doi.org/10.1186/s13661-018-1090-z; MR3877704

[8] T. Laetsch, The number of solutions of a nonlinear two point boundary value problem, *Indiana Univ. Math. J.* **20**(1970), No. 1, 1–13. https://doi.org/10.1512/iumj.1970.20.20001; MR269922

[9] R. M. May, Thresholds and breakpoints in ecosystems with a multiplicity of stable states, *Nature* **269**(1977), 471–477. https://doi.org/10.1038/269471a0

[10] F. J. Odendaal, P. Turchin, F. R. Stermitz, Influence of host-plant density and male harassment on the distribution of female *Euphydryas anicia* (Nymphalidae), *Oecologia* **78**(1989), No. 2, 283–288. https://doi.org/10.1007/BF00377167

[11] A. M. Shapiro, The role of sexual behavior in density-related dispersal of pierid butterflies, *Am. Nat.* **104**(1970), No. 938, 367–372. https://doi.org/10.1086/282670

[12] J. H. Steele, E. W. Henderson, Modeling long term fluctuations in fish stocks, *Science* **224**(1984), 985–987. https://doi.org/10.1126/science.224.4652.985